# Complete substitution of Si for Ti in titanite $Ca(Ti_{1-x}Si_x)^{VI}Si^{IV}O_5$

## R. KNOCHE,* R.J. ANGEL, F. SEIFERT, AND T.F. FLIERVOET[†]

Bayerisches Geoinstitut, Universität Bayreuth, D-95440 Bayreuth, Germany

## ABSTRACT

Phase relations on the join $CaTiSiO_5$-$CaSi_2O_5$ were determined at 1350 °C over the pressure range 3.5–12 GPa by a combination of synthesis and reversal experiments in a piston cylinder and a multi-anvil press. Titanite-like phases were recovered from all experiments in this pressure range. At 3.5 GPa the maximum $Si^{VI}$ content of titanite is 3.0 ± 0.6 mol%, whereas bulk compositions with higher Si content yield a mixture of titanite solid solution plus coesite and walstromite-structured $CaSiO_3$. The maximum $Si^{VI}$ content of the titanite increases with pressure to 21 ± 2 mol% at 7 GPa and 46 ± 2 mol% at 7.5 GPa. At pressures of 8.5 to 12 GPa all intermediate compositions yield a single titanite phase. X-ray and TEM analysis show that these have the $A2/a$ symmetry of the titanite aristotype. The variations of the room-pressure unit-cell parameters of the $A2/a$ phases with composition can be described by the equations $a$ [Å] = 7.040(9) − 0.492(15) $X$($Si^{VI}$); $b$ [Å] = 8.713(7) − 0.316(11) $X$($Si^{VI}$); $c$ [Å] = 6.564(4) − 0.220(7) $X$($Si^{VI}$); β [°] = 113.721(6) − 0.537(12) $X^2$($Si^{VI}$); $V$ (cell) [Å³] = 367.8(9) − 47.5(1.6) $X$($Si^{VI}$). For the $CaSi_2O_5$ composition the recovered material has $I\bar{1}$ symmetry but is known to transform back to $A2/a$ titanite structure at 0.2 GPa at room temperature. Similarly, with increasing pressure the $P2_1/a$ $CaTiSiO_5$ transforms to $A2/a$ symmetry at 3.6 GPa at room temperature. The conclusion is that at 1350 °C and pressures in excess of 8.5 GPa there is complete solid solution between $CaTiSiO_5$ and $CaSi_2O_5$ based upon the isovalent exchange of Si for Ti in the octahedral site of the $A2/a$ structure. Rietveld structure analysis of intermediate compositions reveals no evidence for ordering or intermediate phases. Preliminary experiments at pressures between 13.5 GPa and 16 GPa yielded mixtures of titanite solid solution plus perovskite and stishovite. From these data and information on the phase relations for the $CaSiO_3$-$CaTiO_3$ join the topology of the phase relations between ~3 and ~13 GPa in the central part of the $CaO$-$TiO_2$-$SiO_2$ ternary have been deduced.

## INTRODUCTION

An important mechanism for phase transitions in the silicates of the Earth's mantle is the change of the coordination of Si by oxygen from four (tetrahedral) to six (octahedral) with increasing pressure. In chemically complex systems (e.g., $KAlSi_3O_8$, Kinomura et al. 1975) the increase in Si coordination often proceeds through a sequence of polymorphic transitions or reactions to intermediate phases that contain Si in both coordinations. An alternative, but little investigated, mechanism for the development of mixed-coordination phases is the continuous substitution of Si for other octahedral cations in silicates containing $SiO_4$ tetrahedra. Examples include the solution of a majorite component into pyrope garnet (Akaogi and Akimoto 1977) and the solution of a Na-Mg-pyroxene component (itself a mixed-coordination

phase; Angel et al. 1988) into clinopyroxenes at high pressures (Gasparik 1989). In the latter example, the solubility appears to be limited to a few mole percents (Gasparik 1989), whereas the system majorite-pyrope is complicated by a second-order phase transition (Heinemann et al. 1997). In both cases, octahedrally coordinated silicon is introduced into the structure by a coupled substitution ($Si^{4+}$ + $Mg^{2+}$ → 2 $Al^{3+}$ in the garnets, and $Si^{4+}$ + 2$Na^+$ → 3 $Mg^{2+}$ in the pyroxene), which naturally leads to ordering and possibly exsolution.

However, the recent discovery of a titanite-structured phase of $CaSi^{VI}Si^{IV}O_5$ (Angel 1997), and the wide stability field in pressure and temperature of titanite, $CaTi^{VI}Si^{IV}O_5$, immediately suggests the possibility of a solid solution between the two end-members in which mixed-coordination of Si would evolve as a result of the isovalent substitution of Si for Ti. Kubo et al. (1997) recently reported the recovery of titanites with compositions ranging from $CaSiSiO_5$ to $Ca(Ti_{0.22}Si_{0.78})SiO_5$ in the system $CaSiO_3$-$CaTiO_3$. We therefore examined the phase relations of the $CaTiSiO_5$-$CaSi_2O_5$ join and characterized the structural state of the titanites synthesized.

---

* Current address: Institut für Mineralogie und Petrographie, Universität Innsbruck, Innrain 52, A-6020 Innsbruck, Austria. E-mail:Ruth.Knoche@uibk.ac.at

† Current address: Phillips Electron Optics, Building AAE, Achtseweg Noord 5, P.O. Box 218, 5651 GG Eindhoven, Netherlands.

**TABLE 1.** Starting materials

| Number | Nominal composition | Microprobe analysis | Comments |
|---|---|---|---|
| S1 | $CaSi_2O_5$ | Si = 2.01(14); Ca = 0.98(30) | Glass* |
| S2 | $CaTiSiO_5$ | | Crystalline*† |
| S3 | $CaTi_{0.5}Si_{1.5}O_5$ | Si = 1.45(2); Ca = 1.03(1); Ti = 0.53(1) | Glass* |
| S4 | $CaTi_{0.25}Si_{1.75}O_5$ | see H-629 | Glass* |
| S5 | $CaTi_{0.1}Si_{1.9}O_5$ | Si = 1.90(3); Ca = 1.00(6); Ti = 0.10(1) | Glass—prepared from S1 and S2* |
| S6 | $CaTi_{0.75}Si_{1.25}O_5$ | see H-713 | Mechanical mixture from S2 and S3 |
| S7 | $CaSiO_3$ + coesite | — | ‡ |

   * A mechanical mixture from $CaCO_3$ (Ventron, 99.998%, dried at 600 °C) and $SiO_2$ (Alpha, 99.99%, dried at 1200 °C) was slowly heated to 1200 °C to drive off the $CO_2$. $TiO_2$ (Aldrich, 99.99%, dried at 1000 °C) was added for Ti-bearing glasses. Mixtures were fused at 1650 °C, ground and refused three times, and quenched to a glass. Ti-poor glasses were turbid because of liquid unmixing on a micron scale, but amorphous to X-rays.
   † Synthesized by devitrifying glass of the same composition.
   ‡ Crystallized from S1 in the piston cylinder apparatus (3.2 GPa, 1000 °C, 23 h) using a Ag-capsule with ~2 wt% $H_2O$.

## EXPERIMENTS AND ANALYSES

Seven different starting materials were prepared; their compositions and method of preparation are reported in Table 1 together with the experimental conditions and the analytical results.

Experiments at pressures between 6 and 16 GPa were performed in a 1000 ton split-sphere, multi-anvil apparatus. The pressure cell consisted of a MgO octahedron with either 18 mm edge length (6–11 GPa) or 14 mm edge length (>11 GPa) and contained a cylindrical $LaCrO_3$ resistance heater with a stepped wall to minimize the temperature gradient along the length of the sample. The powdered starting material was surrounded by two layers of rhenium foil (25 μm thickness), which were formed into a cylindrical shape. The temperature gradient within the sample is estimated to be <40 °C in the assembly used at 6–11 GPa and <70 °C in the assembly used above 11 GPa. The maximum uncertainty in pres-

sure is estimated to be ±0.5 GPa. For details of the cell and pressure calibration as well as the general setup of the high-pressure multi-anvil device see Rubie et al. (1993a, 1993b) and Schmidt (1995). For all experiments the cell assembly was compressed at room temperature to a desired final oil pressure and then heated at 100 °C/min to the final temperature of 1350 °C. During the experiments temperature was measured and controlled with a WRe25-WRe3 thermocouple at the top of the capsule. The sample was kept at 1350 ± 2 °C and then quenched to <300 °C within 3 s by shutting off the voltage supply.

One experiment at 3.5 GPa (PC-I, Table 2) was performed in a piston-cylinder apparatus using a ½″ talc-pyrex assembly with a tapered graphite furnace. The powdered sample was contained in a platinum capsule. The temperature gradient within the sample was <10 °C. The pressure calibration is accurate to ±0.1 GPa when friction corrections based upon the standard reactions re-

**TABLE 2.** Experimental conditions, starting material, product phases, and titanite compositions $Ca_xTi_ySi_zO_5$

| Number | Pressure (GPa) | Tempera-ture (°C) | Time (h) | Starting material | Phases* | $(Ca_xTi_ySi_zO_5)$† | | |
|---|---|---|---|---|---|---|---|---|
| | | | | | | x | y | z |
| PC-I | 3.5 | 1350 | 6 | S3 | tnt + $CaSiO_3$ + cs | 1.01(1) | 0.97(1) | 1.03(1) |
| H-570 | 6.0 | 1350 | 4 | S3 | tnt + $CaSiO_3$-II + cs | 1.0‡ | 0.84(3)‡ | 1.16(3)‡ |
| H-597 | 7.0 | 1350 | 16 | S2 + S7 | tnt + $CaSiO_3$-II + cs | 0.96(1) | 0.80(2) | 1.22(2) |
| H-575 | 7.5 | 1350 | 4 | S3 | tnt + $CaSiO_3$-II + cs | 1.00(5) | 0.54(4) | 1.46(5) |
| H-567 | 8.5 | 1350 | 4 | S3 | tnt | 0.97(1) | 0.52(2) | 1.50(2) |
| H-568 | 8.5 | 1350 | 4 | S1 | tnt + $CaSiO_3$-II + cs | 1.01(10) | — | 2.00(5) |
| H-713 | 8.5 | 1350 | 8 | S6 | tnt | 1.01(1) | 0.75(2) | 1.24(2) |
| H-561 | 11.0 | 1350 | 4 | S3 | tnt | 1.03(2) | 0.52(2) | 1.47(3) |
| H-629 | 11.0 | 1350 | 4 | S4 | tnt | 0.98(2) | 0.25(1) | 1.76(2) |
| H-653 | 11.0 | 1350 | 4 | S5 | tnt | 1.01(3) | 0.10(1) | 1.90(2) |
| H-608 | 13.5 | 1350 | 4 | S3 | tnt + st + pv | 1.0§ | 0.49§ | 1.51§ |
| H-615 | 14.5 | 1350 | 4 | S3 | st + pv + tnt + glass | 1.0§ | 0.47§ | 1.53§ |
| H-622 | 14.5 | 1350 | 4 | S1 | tnt | ‖ | — | ‖ |
| H-645 | 16.0 | 1350 | 4 | S4 | tnt + pv + st | 1.0§ | 0.20§ | 1.80§ |
| H-590 | 16.0 | 1350 | 4 | S3 | pv + st | — | — | — |

   * As identified by XRD; tnt = titanite solid solution; cs = coesite; st = stishovite; pv = perovskite solid solution.
   † Determined from electron microprobe analysis (15 kV, 15 nA, point electron beam of 1–2 μm; measuring 20 s on sample, 10 s on each background; using wollastonite, $CaSiO_3$, and $MnTiO_3$ as standards).
   ‡ Sample was too fine grained (<1 μm) to determine the titanite composition using the electron microprobe; therefore it was determined from TEM using the method of Van Capellen and Doukhan (1994). KSi-factors at zero thickness for Ca and Ti have been determined on the pure titanite, that for O on forsterite. Relative errors are estimated to be less than 5% (Van Cappellen 1994).
   § Samples are too fine grained to determine single compositions using the electron microprobe; reported compositions are estimated from unit-cell parameters (see Table 3).
   ‖ See analysis of S1 and H-568.

**TABLE 3.** Lattice parameters of $A2/a$ Ca(Ti,Si)$^{VI}$Si$^{IV}$O$_5$ solid solution and of $Fm\bar{3}m$ perovskites

| Number | Si$^{VI}$ of titanite | Titanite | | | | | Perovskite | | |
|---|---|---|---|---|---|---|---|---|---|
| | | $a$ | $b$ | $c$ | $\beta$ | $V$ | $a$ | $V$ | $x^*$ |
| PC-I | 0.03(1) | 7.0200(2) | 8.6946(3) | 6.5461(2) | 113.749(2) | 365.71(2) | | | |
| H-570 | 0.16(3) | 6.9823(2) | 8.6775(2) | 6.5352(2) | 113.704(2) | 362.55(2) | | | |
| H-597 | 0.22(1) | 6.9227(1) | 8.6394(2) | 6.5129(1) | 113.687(1) | 356.71(1) | | | |
| H-713 | 0.24(2) | 6.9066(1) | 8.6308(1) | 6.5077(1) | 113.676(1) | 355.27(1) | | | |
| H-575 | 0.46(5) | 6.8240(2) | 8.5737(2) | 6.4698(2) | 113.620(2) | 346.81(2) | | | |
| H-561 | 0.47(3) | 6.7984(4) | 8.5540(5) | 6.4512(4) | 113.606(4) | 343.76(4) | | | |
| H-567 | 0.50(2) | 6.7885(2) | 8.5463(2) | 6.4510(2) | 113.594(3) | 342.98(2) | | | |
| H-629 | 0.76(2) | 6.6778(5) | 8.4797(6) | 6.4027(5) | 113.431(4) | 332.66(6) | | | |
| H-653 | 0.90(2) | 6.5971(3) | 8.4358(3) | 6.3663(3) | 113.279(2) | 325.45(3) | | | |
| H-608 | 0.51† | 6.786(1) | 8.560(1) | 6.448(1) | 113.50(1) | 343.48(10) | 7.450(2) | 413.6(4) | 0.40 |
| H-615 | 0.53† | 6.774(1) | 8.551(1) | 6.443(1) | 113.48(1) | 342.30(8) | 7.4643(7) | 415.87(11) | 0.37 |
| H-645 | 0.80† | 6.6443(9) | 8.473(1) | 6.378(1) | 113.18(2) | 330.09(7) | 7.5328(7) | 397.5(1) | 0.59 |
| H-590 | | | | | | | 7.4053(3) | 406.10(5) | 0.49 |

\* Ca$_2$Ti$_{1-x}$Si$_x$O$_6$; perovskite compositions determined from unit-cell volume and the relationship given by Kubo et al. (1997).
† Samples are too fine grained to determine single compositions using the electron microprobe; reported compositions are estimated from unit-cell parameters.

ported by Ross et al. (1986), Holland (1980), and Bohlen and Boettcher (1981) are included (Woodland and O'Neill 1993). Heating and quenching rates were similar to those of the multi-anvil experiments.

Following recovery of the samples, identification of the phases of the products of the experiment was performed on the basis of X-ray powder diffraction patterns obtained with a Siemens D5000 diffractometer equipped with a copper sealed-tube X-ray source. Cell parameters of the titanite-like phases (Table 3) were obtained by full-pattern Le-Bail fits (LeBail 1992) of diffraction patterns between 2θ of 15° and 100°. In addition, the structures of the titanite solid solution in four single-phase samples (H-567, H-629, H-653, and H-713) were determined by Rietveld



**FIGURE 1.** Phase relations in the system CaTiSiO$_5$-CaSi$_2$O$_5$. Open circles represent starting compositions that evolved into multiple phases (compositions indicated by arrow heads) in the course of the experiments. Filled circles represent experiments where compositions before and after the experiment were the same. Temperature is 1350 °C.

refinement of the powder patterns. All refinements were performed with the GSAS program package (Larsen and von Dreele 1985).

Some grains of the products from each experiment were mounted in epoxy and prepared for compositional analysis with a Cameca SX50 electron microprobe (Table 2). For transmission electron microscope (TEM) investigations small amounts of samples PC-I and H-570 as well as the pure titanite starting material (S2, Table 1) were crushed in alcohol. The dispersed fine grained (<1 μm) powders were collected on holey-carbon grids for TEM investigations. The observations were carried out on a Philips CM20 FEG operating at 200 kV, with a NORAN Voyager 2 analytical EDS system to facilitate mineral identification. The TEM observations were made in selected area diffraction and microdiffraction modes as well as standard bright-field and dark-field.

## RESULTS AND DISCUSSION

Titanite-like phases were recovered from all of the experiments (Fig. 1), except run H-590 at 16 GPa (Table 2). Samples of the CaSi$_2$O$_5$ end-member recovered from the multi-anvil press exhibit $I\bar{1}$ symmetry and possess a structure that is a derivative of the titanite aristotype structure and contains Si in fivefold coordination by oxygen (Angel et al. 1996). However, the triclinic CaSi$_2$O$_5$ phase undergoes a phase transition at 0.2 GPa back to a titanite structure with $A2/a$ symmetry (Angel 1997), and this is assumed to be the symmetry of CaSi$_2$O$_5$ at synthesis conditions in the multi-anvil press.

By contrast, end-member titanite, CaTiSiO$_5$, has space group symmetry $P2_1/a$ at room temperature and pressure as a result of ordering of the displacements of Ti atoms away from the centers of the TiO$_6$ octahedra. This ordering gives rise to weak but sharp superlattice reflections with indices $k + l$ = odd in the diffraction patterns (e.g., Speer and Gibbs 1976; Taylor and Brown 1976). These
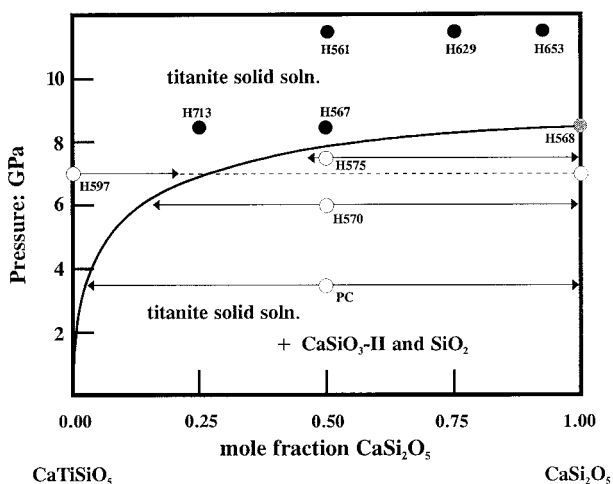
were readily observed in both X-ray powder diffraction patterns and TEM diffraction patterns of $CaTiSiO_5$ (S2).

No superlattice reflections were visible in the powder X-ray diffraction pattern of the titanite phase produced in the run at 3.5 GPa (experiment PC-I) that has 3% of the Ti substituted by octahedral Si, but TEM diffraction patterns exhibited streaks running parallel to $0k0$ and $00l$ in $hk0$ and $h0l$ sections, respectively. These streaks have weak maxima at positions corresponding to super-lattice positions $k + l =$ odd, and they appear to be the result of the intersection of sheets of diffuse intensity with the Ewald sphere. Similar streaks have been observed in diffraction patterns from natural titanites containing Al and Fe substituted for Ti and have been interpreted as arising from the presence of only short-range order of the Ti displacements within the structure (Higgins and Ribbe 1976; Meyer et al. 1996). Titanite itself is known to undergo a symmetry change to $A2/a$ symmetry at high temperatures at room pressure (Kek et al. 1997 and references therein), and at 3.6 GPa at room temperature (Kunz et al. 1996; Angel et al., in preparation). Therefore, we conclude that the ordering in the titanite of PC-I occurred on cooling and/or pressure release from run conditions, and that the symmetry of both the $CaTiSiO_5$ and the titanite in this experiment at 1350 °C and 3.5 GPa was $A2/a$. This interpretation is supported by the careful examination by both TEM and X-ray diffraction of the more Si-rich members of the solid solution. This revealed no evidence for either superlattice reflections or diffuse streaks, and these samples all therefore exhibit $A2/a$ symmetry at room pressure and temperature. High-pressure X-ray powder diffraction of the titanite from experiment H-567 $[X(Si^{VI}) = 0.50(2)]$ revealed no evidence of phase transitions up to a maximum pressure of $\sim$7.5 GPa (Angel et al., in preparation).

Evidence for a continuous solid solution is also provided by the smooth variation of the unit-cell parameters of the titanite phases with composition (Table 3, Fig. 2). These data (except that of experiment PC-I; see below) together with the cell parameters of the $A2/a$ polymorph of $CaSi_2O_5$ itself (Angel 1997) were fitted by least-squares to yield the relationships:

$$a\ [\text{Å}] = 7.040(9) - 0.492(15)X(Si^{VI})$$

$$b\ [\text{Å}] = 8.713(7) - 0.316(11)X(Si^{VI})$$

$$c\ [\text{Å}] = 6.564(4) - 0.220(7)X(Si^{VI})$$

$$\beta\ [°] = 113.721(6) - 0.537(12)X^2(Si^{VI})$$

$$V\ (\text{cell})\ [\text{Å}^3] = 367.8(9) - 47.5(1.6)X(Si^{VI}).$$

Note that the constant terms in each expression are the predicted cell parameters for the titanite end-member with $A2/a$ symmetry at room temperature and pressure. Comparison of these with the observed unit-cell parameters of $P2_1/a$ titanite (e.g., Xirouchakis et al. 1997) reveals that the major metrical change associated with the $P2_1/a$ to $A2/a$ symmetry change with increasing $Si^{VI}$ content is a decrease in the unit-cell angle $\beta$ (Fig. 2). The transition
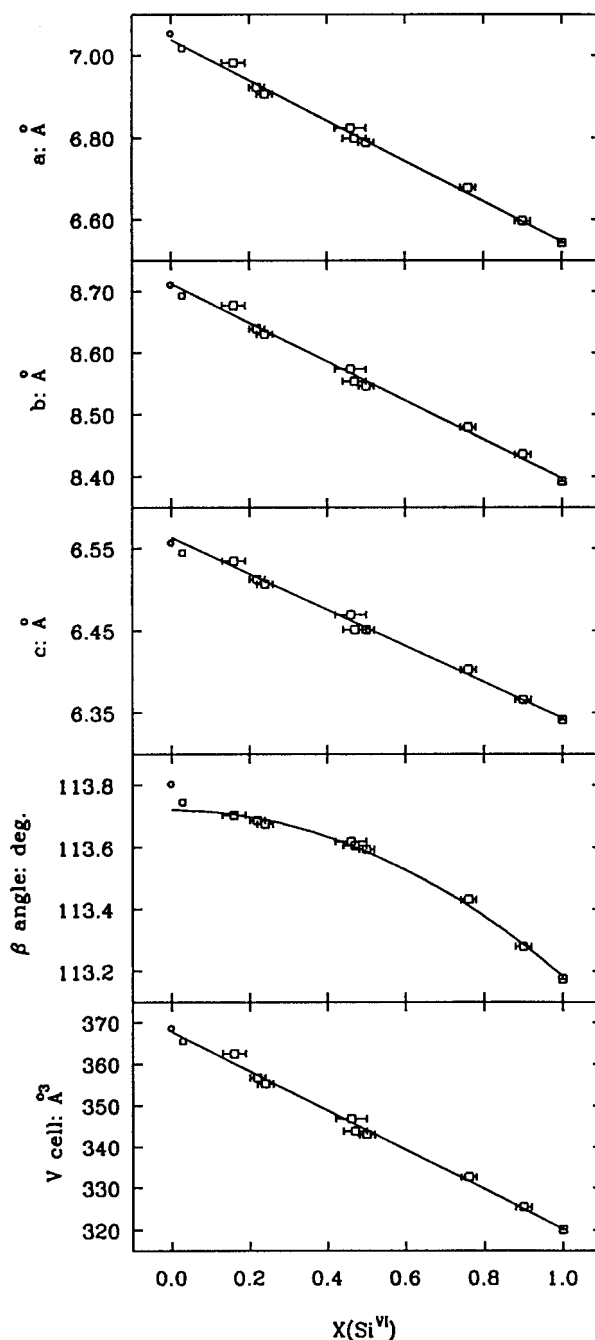


**FIGURE 2.** Unit-cell parameters of the titanite solid solution as determined by Le-Bail fits to the X-ray powder diffraction patterns. Lines represent least-squares fits to the data from samples with $X(Si^{VI}) > 0.1$. Coefficients are reported in the text. The small circles at $X(Si^{VI}) = 0.00$ represent the cell parameters of end-member titanite taken from Xirouchakos et al. (1997). Note that within the resolution of our data, there is no evidence for any excess volume of mixing in the solid solution.
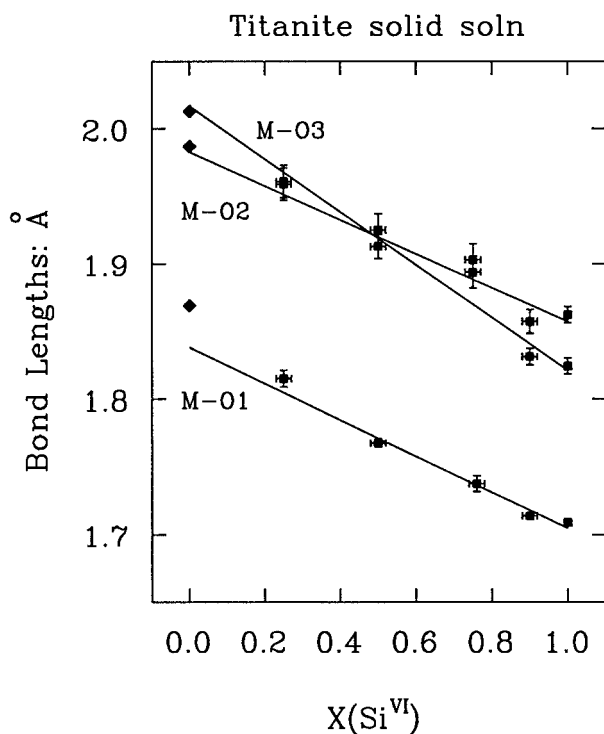
## Titanite solid soln



**FIGURE 3.** Variation of M-O bond lengths across the titanite solid solution. Vertical error bars represent 3 σ uncertainties in bond lengths. For end-member $P2_1/a$ titanite the average of pairs of bond lengths are plotted. Data for $A2/a$ $CaSi_2O_5$ from Angel (1997). Lines are linear fits to all $A2/a$ data.

can therefore be described in terms of a shear of the unit cell in the (010) plane. The value of the angle β of the titanite from experiment PC-I is intermediate between the trend for the $A2/a$ samples and that of the end-member $CaTiSiO_5$, which is consistent with the intermediate structural state of this sample revealed by our TEM observations.

The structures of four of the single-phase titanites of intermediate compositions, as determined by Rietveld refinement, show no significant variations from linear trends with composition (Fig. 3). As expected, the substitution of Si for Ti on the octahedrally coordinated M site results in a decrease in M-O bond lengths from their average values in titanite. The M-O1-M angle, which measures the relative tilting of consecutive octahedra in the octahedral chains, increases with increasing Si content and therefore represents a straightening of the chains. This straightening by some 5° across the entire solid solution is accompanied by a small but significant decrease in the average Ca-O bond length, but no significant change of the tetrahedral Si-O bond lengths. All of these trends are the opposite of the effects produced when Ti is substituted by a larger cation such as Sn and represent the response of the titanite structure type to steric strain (Kunz et al. 1997). The continuous nature of these changes with composition is further evidence for absence

of either ordering of Si and Ti on the octahedral sites or of any other discontinuity in the solid solution.

In spite of the varied symmetries displayed by the titanite-like samples at room $P$ and $T$ conditions the evidence from other high-pressure diffraction experiments indicates that all of them possessed $A2/a$ symmetry at the conditions of their formation in the multi-anvil press. Therefore at 1350 °C and pressures in excess of 8.5 GPa a complete solid solution with $A2/a$ symmetry exists between $CaTiSiO_5$ and $CaSi_2O_5$ (Fig. 1). At pressures below 8.5 GPa the $CaSi_2O_5$ end-member decomposes into a mixture of $SiO_2$ coesite and $CaSiO_3$-II (Trojer 1969; Essene 1974; Huang and Wyllie 1975); experiment H-568 at 8.5 GPa was apparently at, or near to, the equilibrium boundary as the products included all three phases. This result is consistent with the preliminary phase diagram for $CaSi_2O_5$ reported by Kanzaki (1994). The breakdown of $CaSi_2O_5$ at lower pressures opens a three-phase field on the $CaTiSiO_5$-$CaSi_2O_5$ join in which Ti-free $SiO_2$ and $CaSiO_3$-II coexist with titanite solid solution. The solvus is bracketed by three unmixing experiments and one reversal (experiment H-597), which indicate that at low pressures of 3.5 GPa the titanite solution can accommodate at least 3 mol% $Si^{VI}$, and this increases to approximately 25 mol% at 7 GPa (Fig. 1).

We also performed several reconnaissance experiments at higher pressures. One experiment at the 50:50 composition and 16 GPa (H-590) yielded stishovite plus a double-perovskite of composition $Ca_2TiSiO_6$. The space group of this perovskite was confirmed by powder diffraction to be $Fm\bar{3}m$ in agreement with Leinenweber and Parise (1997), which implies ordering of the octahedral Si and Ti. Further runs above 12 GPa at various compositions (see Table 2) yielded mixtures of titanite solid solution plus perovskite and stishovite. All of these run products were too fine grained to allow microprobe analysis. Compositions of the phases were therefore estimated from unit-cell parameters determined by X-ray powder diffraction (Table 3). These data are sufficient to indicate that for Si-rich compositions a Si-enriched $A2/a$ titanite solid-solution co-exists with a perovskite with a lower $Si^{VI}/Ti$ ratio and intermediate between $CaSiO_3$ and $CaTiO_3$. With the exception of experiment H-645, the presence of cell-doubling peaks in the powder diffraction patterns indicates that these perovskites have $Fm\bar{3}m$ symmetry. However, phase relations will be complicated by phase transitions and order/disorder behavior in the perovskite, and further studies are needed to determine both the topology of the phase relations and the precise locations of the phase boundaries.

### PHASE RELATIONS

Our results show that at sufficiently high pressures and temperatures a complete solid solution exists between $CaTiSiO_5$ titanite and $CaSiSiO_5$, based upon the exchange of Si for Ti in the octahedral site of the structure. This substitution appears to occur without ordering of the octahedral cations and the continuous nature of the solid
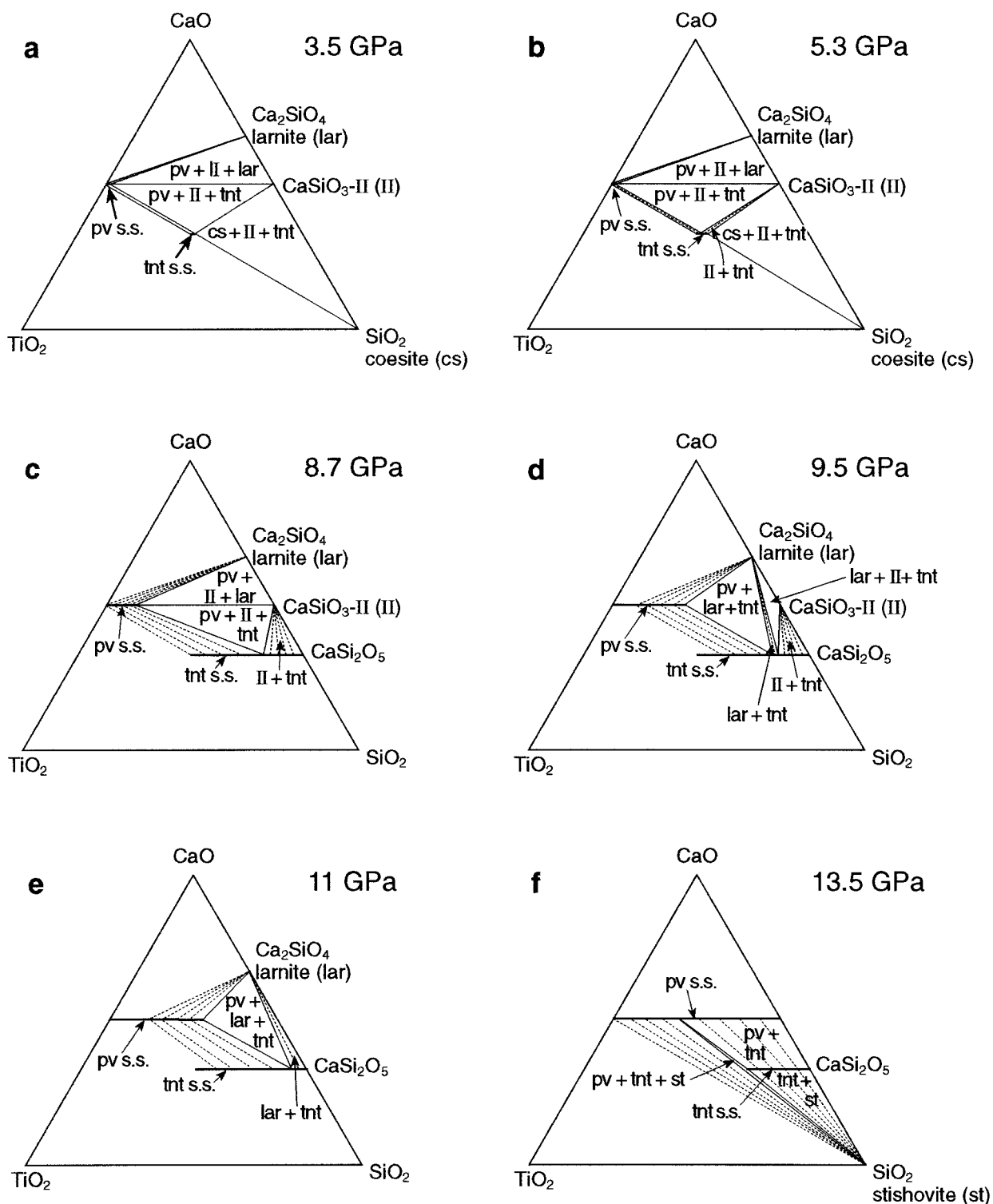
**FIGURE 4.** Topology of the phase equilibria in the central part of the CaO-TiO$_2$-SiO$_2$ ternary at six pressures from ~3.5 GPa to ~13.5 GPa constructed from the results of the current study (at 1350 °C) and the results of Kubo et al. (1997) at 1200 °C. No corrections were made for effects of this temperature difference on the phase stabilities, and pressures are approximate. Tie lines in two-phase fields are consistent with the available data but otherwise schematic. Areas in which insufficient data are available have been left blank. Abbreviations: tnt s.s. = titanite solid solution; pv s.s. = perovskite solid solution; lar = CaSi$_2$O$_4$-larnite; II = walstromite-structured CaSiO$_3$; cs = SiO$_2$-coesite; st = SiO$_2$-stishovite.

solution allows the amount of octahedral silicon in the titanite structure to increase continuously with increasing pressure. At room pressure and temperature the titanite from experiment H-570 with $X(Si^{VI}) = 0.16(3)$ had $A2/a$ symmetry, while even the titanite with $X(Si^{VI}) = 0.03(1)$ from experiment PC-I had very weak super-lattice reflections. This suggests that substitution of perhaps as little as 10 mol% of the Ti by $Si^{VI}$ is sufficient to completely suppress the long-range ordering of the displacements of the Ti cations, the same level as required when Sn is substituted for Ti (Kunz et al. 1997). Because the ionic radius of $Si^{VI}$ is smaller than $Ti^{VI}$, whereas $Sn^{VI}$ is larger (Shannon 1976), these results imply that, as originally suggested by Higgins and Ribbe (1976), the suppression of the $A2/a$ to $P2_1/a$ transition is purely a dilution effect rather than a steric one.

Kubo et al. (1997) recently determined the phase relations on the $CaSiO_3$-$CaTiO_3$ join at 1200 °C at pressures between 5.3 and 13.6 GPa. If we assume that the effects of the 150 °C temperature difference between their experiments and ours are small, we can now use the results reported in this paper and those of Kubo et al. (1997) to deduce the general topology of the phase relations between ~3.5 and ~13.5 GPa in the central part of the $CaO$-$TiO_2$-$SiO_2$ ternary (Fig. 4). At the lowest pressures of ~3.5 GPa both the titanite and perovskite solid solutions are extremely limited in composition, and the ternary therefore consists essentially of a set of three-phase fields (Fig. 4a). With increasing pressure the extent of $Si^{VI}$ substitution for Ti in both the perovskite and the titanite increases, resulting in the expansion of two-phase fields in the ternary diagram (e.g., Fig. 4b). The first change in the topology of the phase relations occurs on increasing pressure at 8.5 GPa (for 1350 °C) when the $CaSi_2O_5$ becomes stable with respect to the mixture $CaSiO_3$-II plus $SiO_2$ (Kanzaki 1994) and the titanite solid solution becomes complete (Fig. 1). At pressures just above this reaction boundary (Fig. 4c) the stable phase assemblage on the silica-rich side of the $CaSiO_3$-$CaTiO_3$ join remains perovskite solid-solution plus $CaSiO_3$-II (Kubo et al. 1997), but at 9.3 GPa (at 1200 °C) perovskite plus $CaSiO_3$-II react to titanite plus $CaSi_2O_4$-larnite and an additional two-phase field develops, as in Figure 4d. This is quickly followed at ~10 GPa (at 1200 °C) by the final breakdown of $CaSiO_3$-II to $Ca_2SiO_4$-larnite plus $CaSi_2O_5$ (Gasparik et al. 1994; Kubo et al. 1997), producing the topology of Figure 4e. At this pressure, the phase assemblages observed on the $CaSiO_3$-$CaTiO_3$ join with increasing Si content are (1) perovskite s.s., (2) perovskite s.s. + titanite s.s. + larnite, and (3) titanite s.s. + larnite (Kubo et al. 1997). Finally, above 12 GPa, $CaSiO_3$ is stable with respect to a mixture of $Ca_2SiO_4$-larnite plus $CaSi_2O_5$ (Gasparik et al. 1994; Wang and Weidner 1994; Kubo et al. 1997), and the perovskite solid solution becomes continuous between $CaSiO_3$ and $CaTiO_3$ (ignoring possible phase transitions associated with Si,Ti ordering, Leinenweber et al. 1997). The extent of the titanite solid solution becomes restricted at the Ti-rich end as Ti-rich compositions are replaced by the assemblage perovskite + $SiO_2$ stishovite (Fig. 4f).

Near end-member titanite is an important minor constituent in many rocks of crustal or even upper mantle origin. According to our results, the incorporation of octahedral silicon becomes significant at fairly low pressures (ca. 3 mol% $CaSiSiO_5$ component at 3.5 GPa and 1350 8C, Table 2). From the positive $PT$-slope of the coesite + wollastonite II → $Ca_2Si_2O_5$ reaction (Kanzaki 1994) we would expect that the solubility of the $Ca_2Si_2O_5$ component in titanite even increases with decreasing temperatures, which are more appropriate to the natural environment. It is therefore likely that partial Ti-Si substitution may also be observed in natural rocks of high-pressure origin, provided the activities of $SiO_2$ and $CaSiO_3$ are high. This combination of conditions exists: For instance, Klemd et al. (1994) described the paragenesis of titanite with quartz and diopside formed near 630 8C and a minimum pressure of 3.1 GPa.

## REFERENCES CITED

Akaogi, M. and Akimoto, S. (1977) Pyroxene-garnet solid solution equilibria in the system $Mg_4Si_4O_{12}$-$Mg_3Al_2Si_3O_{12}$ and $Fe_4Si_4O_{12}$-$Fe_3Al_2Si_3O_{12}$ at high pressures and temperatures. Physics of the Earth and Planetary Interiors, 15, 90–106.

Angel, R.J. (1997) Transformation of fivefold-coordinated silicon to octahedral silicon in calcium silicate, $CaSi_2O_5$. American Mineralogist, 82, 836–839.

Angel, R.J., Gasparik, T., Ross, N.L., Finger, L.W., Prewitt, C.T., and Hazen, R.M. (1988) A silica-rich sodium pyroxene phase with six-coordinated silicon. Nature, 335, 156–158.

Angel, R.J., Ross, N.L., Seifert, F., and Fliervoet, T.F. (1996) Structural characterisation of pentacoordinate silicon in a calcium silicate. Nature, 384, 441–444.

Bohlen, S.R. and Boettcher, A.L. (1981) Experimental investigations and geological applications of orthopyroxene geobarometry. American Mineralogist, 66, 951–964.

Essene, E. (1974) High-pressure transformations in $CaSiO_3$. Contributions to Mineralogy and Petrology, 45, 147–150.

Gasparik, T. (1989) Transformation of enstatite-diopside-jadeite pyroxenes to garnet. Contributions to Mineralogy and Petrology, 102, 389–405.

Gasparik, T., Wolf, K., and Smith, C.M. (1994) Experimental determination of phase relations in the $CaSiO_3$ system from 8 to 15 GPa. American Mineralogist, 79, 1219–1222.

Heinemann, S., Sharp, T.G., Seifert, F., and Rubie, D.C. (1997) The cubic-tetragonal phase transition in the system majorite ($Mg_4Si_4O_{12}$)-pyrope ($Mg_3Al_2Si_3O_{12}$), and garnet symmetry in the Earth's transition zone. Physics and Chemistry of Minerals, 24, 206–221.

Higgins, J.B. and Ribbe, P.H. (1976) The crystal chemistry and space groups of natural and synthetic titanites. American Mineralogist, 61, 878–888.

Holland, T.J.B. (1980) The reaction albite = jadeite + quartz determined experimentally in the range 600–1200 °C. American Mineralogist, 65, 129–134.

Huang, W.-L. and Wyllie, P.J. (1975) Melting and sub-solidus phase relationships for $CaSiO_3$ to 35 kilobars pressure. American Mineralogist, 60, 213–217.

Kanzaki, M. (1994) High-pressure phase equilibrium of the system

$CaSi_2O_5$. Reviews of High Pressure Science and Technology, 3, 217 (in Japanese).

Kek, S., Aroyo, M., Bismayer, U., Schmidt, C., Eichhorn, K., and Krane, H.G. (1997) The two-step phase transition of titanite, $CaTiSiO_5$: a synchrotron radiation study. Zeitschrift für Kristallographie, 212, 9–19.

Kinomura, N., Kume, S., and Koizumi, M. (1975) Synthesis of $K_2Si_4O_9$ with silicon in 4- and 6-coordination. Mineralogical Magazine, 40, 401–404.

Klemd, R., Matthes, S., and Schössler, U. (1994) Reaction textures and fluid behaviour in very high-pressure calc-silicate rocks of the Münchberg gneiss complex, Bavaria, Germany. Journal of Metamorphic Geology, 12, 735–745.

Kubo, A., Suzuki, T., and Akaogi, M. (1997) High-pressure phase equilibria in the system $CaTiO_3$-$CaSiO_3$: stability of perovskite solid solutions. Physics and Chemistry of Minerals, 24, 488–494.

Kunz, M., Xirouchakis, D., Lindsley, D.H., and Häussermann, D. (1996) High-pressure phase transition in titanite ($CaTiOSiO_4$). American Mineralogist, 81, 1527–1530.

Kunz, M., Xirouchakis, D., Wang, Y., Parise, J.B., and Lindsley, D.H. (1997) Structural investigations along the join $CaTiOSiO_4$-$CaSnOSiO_4$. Schweizerische Mineralogisch-Petrographische Mitteilungen, 77, 1–11.

Larsen, A.C. and von Dreele, R.B. (1985) General Structure Analysis System (GSAS). Los Alamos National Laboratory Report LAUR B6–748. Los Alamos, New Mexico.

LeBail, A. (1992) Extracting structure factors from powder diffraction data by iterative full pattern profile fitting. In E. Prince and J.K. Staljek, Eds., Accuracy in powder diffraction II, Special publication 846, National Institute of Standards and Technology, p. 213. Gaithersburg, Maryland.

Leinenweber, K. and Parise, J. (1997) Rietveld refinement of $Ca_2TiSiO_6$ perovskite. American Mineralogist, 82, 475–478.

Leinenweber, K., Grzechnik, A., Voorhees, M., Navrotsky, A., Yao, A., and McMillan, P.F. (1997) Structural variation in $Ca(Ti_xSi_{1-x})O_3$ perovskites ($1 > x > 0.65$) and the ordered phase $Ca_2TiSiO_6$. Physics and Chemistry of Minerals, 24, 528–534.

Meyer, H.W., Zhang, M., Bismayer, U., Salje, E.K.H., Schmidt, C., Kek, S., Morgenroth, W., and Bleser, T. (1996) Phase transformation behaviour of natural titanite: An infra-red, Raman, birefringence and X-ray diffraction study. Phase Transitions, 59, 39–60.

Ross, N.L., Akaogi, M., Navrotsky, A, Susaki, J.-I., and McMillan, P. (1986) Phase transitions among the $CaGeO_3$ polymorphs (Wollastonite, Garnet, and Perovskite Structures): Studies by high-pressure synthesis, high-temperature calorimetry and vibrational spectroscopy and calculation. Journal of Geophysical Research, 91, 4685–4696.

Rubie, D.C., Ross, C.R., Carroll, M.R., and Elphick, S.C. (1993a) Oxygen self-diffusion in $Na_2Si_4O_9$ liquid up to 10 GPa and estimation of high-pressure melt viscosities. American Mineralogist, 78, 574–582.

Rubie, D.C., Karato, S., Yan, H., and O'Neill, H.St.C. (1993b) Low differential stress and controlled chemical environment in multianvil high-pressure experiments. Physics and Chemistry of Minerals, 20, 315–322.

Schmidt, M.W. (1995) Lawsonite: Upper pressure stability and formation of higher density hydrous phases. American Mineralogist, 80, 1286–1292.

Shannon, R.D. (1976) Revised effective ionic radii and systematic studies of interatomic distances in halides and chalcogenides. Acta Crystallographica, A32, 751–767.

Speer, J.A. and Gibbs, G.V. (1976) The crystal structure of synthetic titanite, $CaTiOSiO_4$, and the domain textures of natural titanites. American Mineralogist, 61, 238–247.

Taylor, M. and Brown, G.E. (1976) High-temperature structural study of the $P2_1/a = A2/a$ phase transition in synthetic titanite, $CaTiSiO_5$. American Mineralogist, 61, 435–447.

Trojer, F.J. (1969) The crystal structure of a high-pressure polymorph of $CaSiO_3$. Zeitschrift für Kristallographie, 130, 185–206.

Van Capellen, E. (1994) Practical hints for the parameterless correction (or extrapolation) method in transmission X-ray microanalysis. Philips Electron Optics Internal Report.

Van Capellen, E. and Doukhan, J.C. (1994) Quantitative transmission X-ray microanalysis of ionic compounds. Ultramicroscopy, 53, 343–349.

Wang, Y. and Weidner, D.J. (1994) Thermoelasticity of $CaSiO_3$ perovskite and implications for the lower mantle. Geophysical Research Letters, 21, 895–898.

Woodland, A.B. and O'Neill, H.St.C. (1993) Synthesis and stability of $Fe_3^{2+}Fe_2^{3+}Si_3O_{12}$ garnet and phase relations with $Fe_3Al_2Si_3O_{12}$-$Fe_3^{2+}Fe_2^{3+}Si_3O_{12}$ solutions. American Mineralogist, 78, 1002–1015.

Xirouchakos, D., Kunz, M., Parise, J.B., and Lindsley, D.H. (1997) Synthesis methods and unit-cell volume of end-member titanite ($CaTiOSiO_4$). American Mineralogist, 82, 748–753.